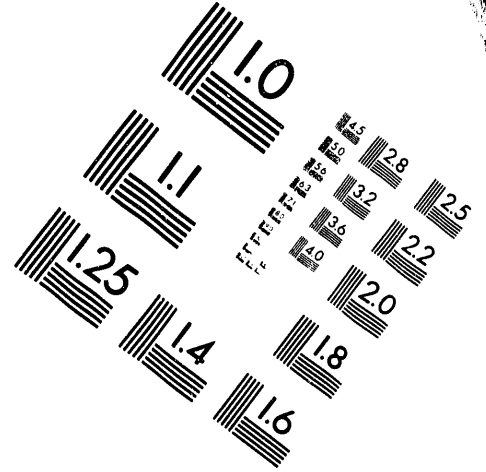
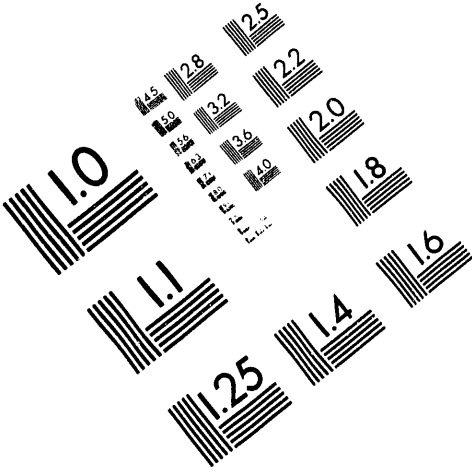




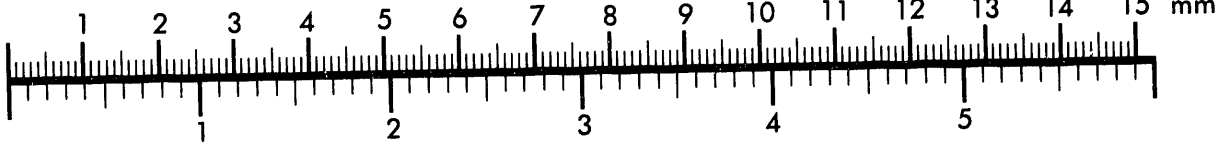
AIM

Association for Information and Image Management

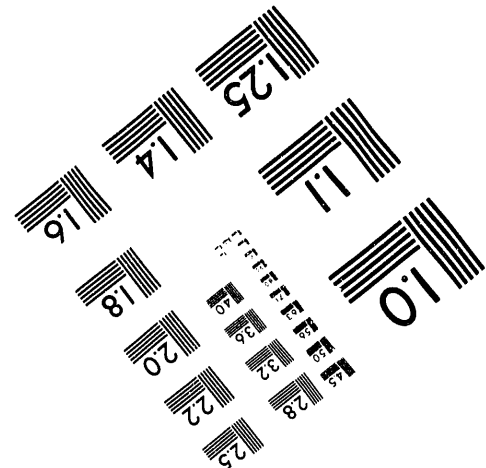
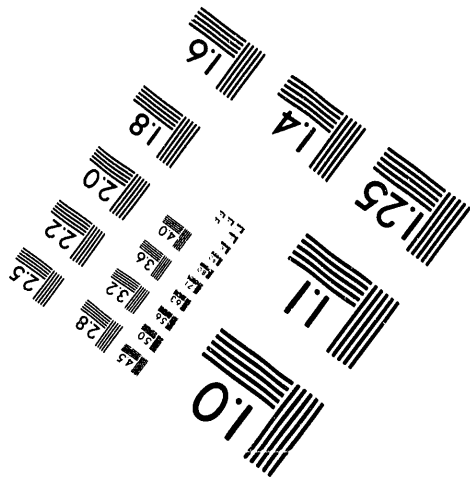
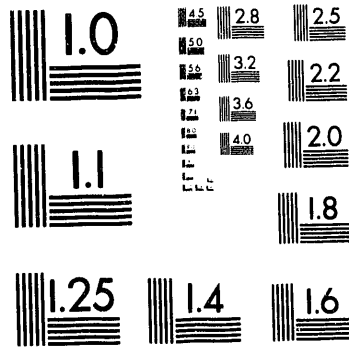
1100 Wayne Avenue, Suite 1100
Silver Spring, Maryland 20910
301/587-8202



Centimeter



Inches



MANUFACTURED TO AIM STANDARDS
BY APPLIED IMAGE, INC.

1 of 1

Conf-930616--5

LA-UR- 93-2354

TITLE:

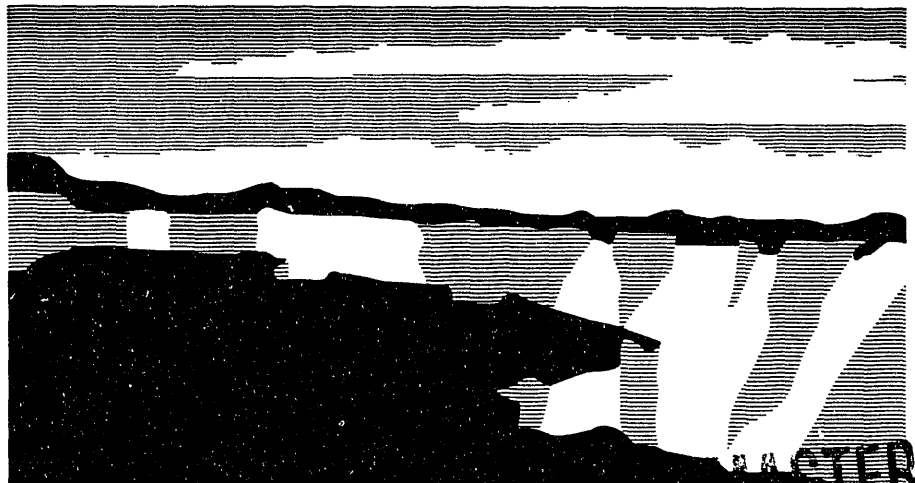
**A MICROSECOND-PULSEWIDTH,
INTENSE, LIGHT-ION BEAM
ACCELERATOR**

AUTHORS:

D. J. Rej, R. R. Bartsch, H. A. Davis,
J. B. Greenly, and W. J. Waganaar

SUBMITTED TO:

*9th IEEE Pulsed Power Conference
Albuquerque, NM
June 21-23, 1993*



Los Alamos
NATIONAL LABORATORY

Los Alamos National Laboratory, an affirmative action/equal opportunity employer, is operated by the University of California for the U.S. Department of Energy under contract W-7405-ENG-36. By acceptance of this article, the publisher recognizes that the U.S. Government retains a nonexclusive, royalty-free license to publish or reproduce the published form of this contribution, or to allow others to do so, for U.S. Government purposes. The Los Alamos National Laboratory requests that the publisher identify this article as work performed under the auspices of the U.S. Department of Energy.

Form No. 836 R5
ST 2629 10/91

DISTRIBUTION OF THIS DOCUMENT IS UNLIMITED

ce

A MICROSECOND-PULSEWIDTH, INTENSE, LIGHT-ION BEAM ACCELERATOR

D. J. Rej, R. R. Bartsch, H. A. Davis, J. B. Greenly,* W. J. Wagenaar

Physics Division, MS-E526, Los Alamos National Laboratory, Los Alamos, NM 87545

Abstract

A relatively long-pulsewidth (0.1-1 μ s) intense ion beam accelerator has been built for materials processing applications. An applied- B_r , magnetically-insulated extraction ion diode with dielectric flashover ion source is installed directly onto the output of a 1.2-MV, 300-kJ Marx generator. Initial operation of the accelerator at 0.4 MV indicates satisfactory performance without the need for additional pulse-shaping.

Introduction

Over the last two decades, there has been remarkable progress in the understanding and development of intense, pulsed ion beams.^{1,2} The primary application driving the development of this technology is inertial confinement fusion (ICF) energy research.³ Recently, however, several novel materials processing applications utilizing intense ion beam technology have emerged. Because of the short range of ions in matter, applications usually involve the surface modification of materials, *e.g.*, implantation,⁴ alloy mixing,^{5,6} defect formation,^{7,8} polishing,⁹ glazing,^{9,10} and thin film deposition.¹¹⁻¹⁴ For many of these applications, the beam acts as a heat source that will rapidly melt or evaporate a target material surface. Consequently, long-pulsewidth intense ion beams are desirable to maximize surface heating with minimum shock waves, provided that thermal conduction into the target during the beam pulse is low. For most materials and 1-MeV beam energies, microsecond-long pulses may be optimal. Thus, materials processing applications could be enhanced by the development of beam pulsewidths greater than the 10-50 ns needed for ICF. In this paper, we report details of a long-pulsewidth, intense, light ion beam driver constructed at Los Alamos National Laboratory, which utilizes an applied- B_r , magnetically-insulated ion diode that is installed directly onto the output of a Marx generator.

The ion diode geometry is shown schematically in Figure 1. Ions are accelerated by a high-voltage pulse applied across an annular anode-cathode (A-K) gap located in vacuum. Undesirable currents from field-emitted cathode electrons are suppressed by an applied radial magnetic field B_r . The field is generated by pulsed electromagnets (shown in the schematic as two concentric coils on the cathode side) and flux-excluding metal components located in the vacuum chamber. The electrons are confined in a sheath, thereby forming a virtual cathode which can enhance the local accelerating electric field and reduce the ion space charge; consequently, ion diodes are intrinsically high-power-density devices, capable of operating with ion current density enhancement factors 10 to 100-times the Child-Langmuir space-charge limit for the vacuum condition.^{15,16} The applied- B_r configuration in Fig. 1 is also known as an "extraction diode" since the accelerated beam can exit the diode region; subsequently, the beam may be focussed and propagated, provided there are sufficient space-charge-neutralizing electrons downstream. The cylindrically-symmetric geometry is desirable since the electron $\mathbf{E} \times \mathbf{B}$ drift trajectories may remain confined in the A-K gap, thereby minimizing the electron current and enhancing the ion current density. For optimum performance with the dielectric anode ion sources used here, B_r is usually set to about 1.5-times the critical field needed to confine the accelerated electrons in the A-K gap. The extraction geometry

is attractive since relatively long ion beam pulsewidths, desirable for several materials processing applications, may be obtained. In contrast, non-axisymmetric diode configurations have large asymmetric plasma production caused by electron bombardment along one side of the A-K gap.¹⁷ Expansion of this plasma may prematurely close the gap, thus limiting the overall useable pulsewidth.

A relatively simple and common anode ion source uses the surface breakdown of a solid dielectric attached to a metallic anode. Sheath electrons diffuse across the A-K gap from the cathode and bombard the anode surface to produce a plasma. Plasma generation is believed to be initiated by dielectric breakdown induced by the excess negative charge of accelerated electrons which accumulate in the anode surface. More advanced ion sources have also been developed. For example, anodes constructed from condensed gases on cryogenic surfaces,¹⁸ and gas-loaded metallic foils,¹⁹ have resulted in high-purity proton and deuteron beams. Also, active plasma sources using localized gas injection and breakdown before application of the accelerating voltage have been developed to produce a pure, reproducible beam capable of high repetition rate and long hardware lifetime.²⁰

The intense ion beam device discussed in this paper is an extension of earlier work involving microsecond pulsewidth accelerators, which were developed for magnetic fusion applications and utilized both the extraction diode geometry at 100-kV voltages,²¹ and the cylindrical "barrel diode" configuration at 1 MV voltages.²²

Ion Diode Design

The extraction diode that has been developed is illustrated in Figure 2. The magnet coils are positioned on the cathode side, rather than on the anode side, for several reasons. First, the cathode is electrically grounded, so there is no need for high-voltage isolation of the coils from their power supply. Second, electrons field emitted from the cathode tips connect to field lines which do not intersect high-voltage anode structures (Fig. 3). This is important to avoid electron leakage currents and to build up an adequate virtual cathode in the A-K gap. Third, there is minimum net magnetic deflection of ions. The beam propagates through the return magnet flux, thereby conserving canonical angular momentum. In other words, the impulse imparted by the return flux counteracts the $\mathbf{v}_z \times \mathbf{B}_r$ force imparted on the ions as they accelerate across the A-K gap. A potential problem with this configuration is in the magnetized drift region between cathode cylinders. Electrons remain magnetically insulated and are not free to stream with the ion beam in this region; thus, space-charge neutralization must be provided, for example by external gas injection²³ or from wall emission.

The dielectric "flashover" anode consists of a Lucite annulus, 194-mm i.d., 292-mm o.d., 6.4-mm thick, mounted concentrically onto an aluminum high-voltage electrode. Both solid and perforated (with 712 evenly-spaced, 0.8-mm diameter holes) anodes have been used. Based on previous operating experience, the beam constituency is expected to be a mixture of the elements found in the anode, H, C, and O. The cathode consists of two concentric cylinders constructed from Ti-8Al-1Mo-1V alloy, each 102-mm

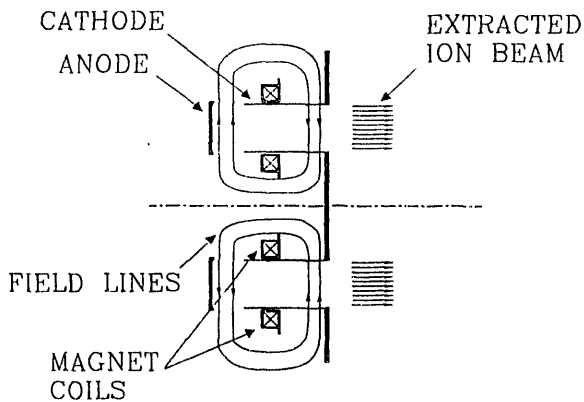


Fig. 1: Schematic drawing of an applied- B_r extraction diode.

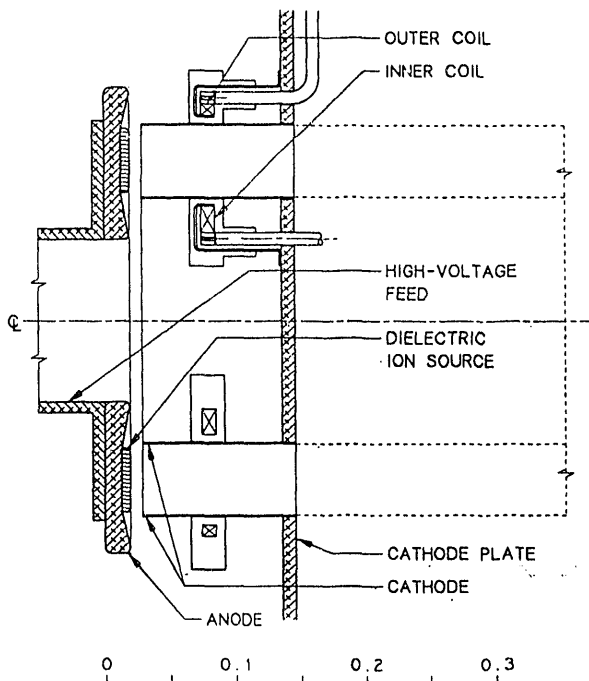


Fig. 2: Intense ion beam diode design. Scale is in meters.

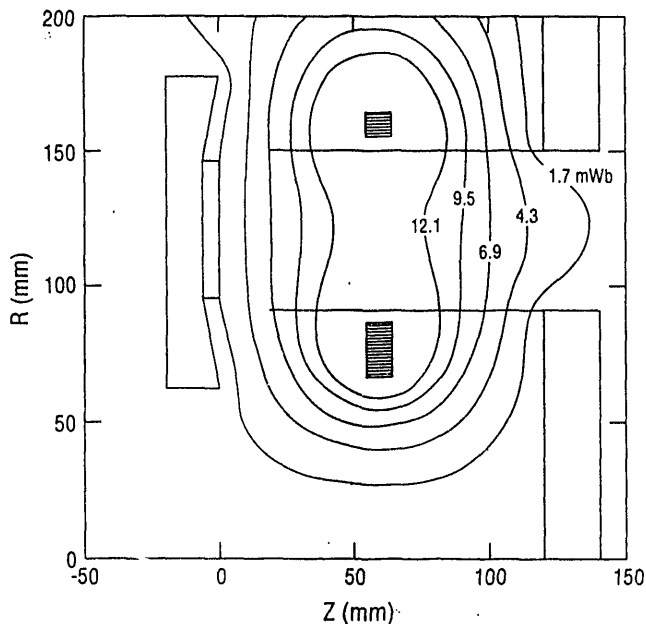


Fig. 3: Vacuum magnetic field flux surfaces in ion diode.

long and 0.8-mm thick with diameters of 186 mm and 298 mm. For these experiments, the anode-cathode gap spacing is 19 mm.

The B_r field is produced by two concentric magnets, 18 turns with a 77-mm mean radius (inner) and 7 turns with 161-mm radius (outer), positioned midway between the anode and an aluminum plate on which the magnets and cathode electrodes are mounted. Each magnet is wound from 0.5-mm thick, 10-mm wide beryllium-copper tape²⁴ which is wrapped with 0.2-mm thickness Kapton film (0.05-mm thick, 13-mm wide film, wrapped in two layers, half lapped) for electrical insulation. The BeCu tape is obtained fully annealed to enable easy wrapping and winding. After being wound, the coils are precipitation hardened in a vacuum oven at 400° C for four hours. Following heat treatment, the high-voltage leads (consisting of the center conductor and insulation of RG 217/U cable) are soldered to the coil. The coils are then wrapped with fiberglass cloth, while the leads are enforced with NEMA G-10 composite. Each magnet assembly is then individually cast in epoxy.²⁵

The magnets are independently powered by 10-kV, 500- μ F capacitors. The coil current risetimes are 170 μ s (outer) and 250 μ s (inner), which are sufficiently long for fields to penetrate the cathode electrodes, but short enough to prevent significant penetration into the aluminum anode electrode. Typical computed vacuum magnetic field flux surfaces and field profiles are shown in Figures 3 and 4, respectively, for 6 kA currents in both coils.

The diode is configured within a vacuum enclosure consisting of aluminum (6061/T6) and stainless-steel (304) chambers. A 2×10^{-6} torr base pressure is obtained with a 0.4-m cryopump. As illustrated in Figure 5, the evacuated assembly may be subdivided into five regions: (1) the high-voltage interface to the Marx generator; (2) the vacuum pump stand; (3) a 0.3-m-long spool that houses an optional plasma opening switch (POS); (4) the applied- B_r ion diode enclosure; and (5) the materials-processing chamber. A photograph of the assembled accelerator is shown in Figure 6.

High-Voltage Power Supply

The ion diode is powered by a 10-stage Marx generator with a 300-kJ output at 1.2 MV. The Marx generator consists of sixty 2.8- μ F, 60-kV capacitors, configured 3 units in parallel to a pack, and 20 packs in series. The entire assembly is contained in dielectric oil for high-voltage insulation. Bipolar charging results in a 120-kV spark gap voltage. All ten spark gaps are triggered by a single 280-kV, 0.8-kJ trigger Marx generator.

The diode is connected directly to the Marx generator through a conventional aluminum/Lucite stacked-ring oil-vacuum interface as shown in Fig. 5. There are no output switches or pulse-forming

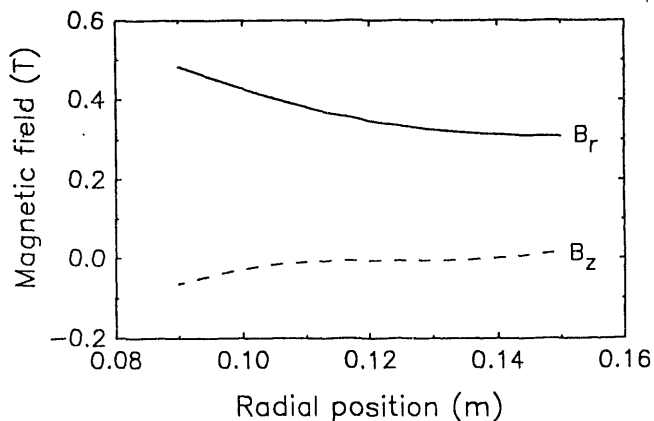


Fig. 4: Magnetic field as a function of radial position inside A-K gap.

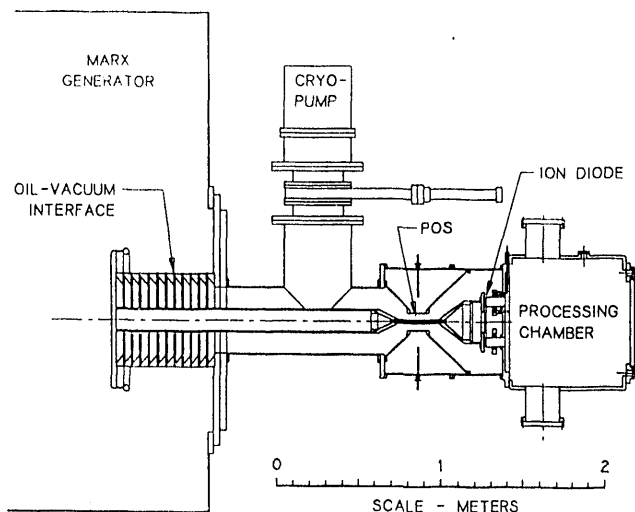


Fig. 5: Assembly drawing of ion beam generator.

lines, although a plasma opening switch (POS) has been constructed for future experiments to shape the diode voltage pulse. The combined source inductance of the Marx/interface/diode configuration is approximately $3 \mu\text{H}$. A $1.6\text{-}\Omega$ series resistance is installed between the Marx output and the vacuum interface to limit the output current after A-K gap closure.

Initial Performance

Initial experiments have been performed at Marx erection voltages of approximately 600 kV. Diagnostics include a resistive voltage divider and Rogowski coil, both located near the oil-vacuum interface, to measure Marx voltage and total output current, respectively. These monitors were built and calibrated by the manufacturer²⁶ of the oil-vacuum interface. The $10^4:1$ voltage divider was calibrated to $\pm 3\%$ accuracy. The Rogowski coil was calibrated *in-situ* with its passive integrator to $\pm 7\%$.

Ion current densities j_i are measured with a radial array of four Faraday cups placed near one azimuthal location at an axial position 138 mm from the anode. The Faraday cup design utilizes a recommended geometry,²⁷ and consists of a Elkonite collector aligned behind a 0.5-mm-diameter entrance aperture. The collector detects ions over a 394 mrad acceptance angle which is about two-times larger than typical beam divergences. To suppress electrons that stream with the ion beam, the collector has been operated at negative bias voltages up to 600 V. The theories of biased Faraday cup operation for intense ion beams reveal that secondary electron emission from the collector to the grounded housing may be neglected.²⁷⁻²⁹ The biased collectors, however, are found unreliable for our accelerator. At approximately 100 to 200 ns into the pulse, a breakdown between collector and ground is observed, presumably caused by a plasma ablated off the collector by the beam. This breakdown results in an erroneously high Faraday cup signal. Electron currents have been suppressed without breakdown on unbiased collectors when a 0.2-T transverse magnetic field is applied over a region ± 1 cm around the entrance aperture. The field is produced by two SmCo permanent magnets positioned on the outer surface of the Faraday cup housing. Several phenomenon can cause errors in Faraday cup measurements. For example, j_i may be underestimated if electrons are not completely filtered from the beam, or if a high-density plasma ablated near the entrance aperture attenuates ions. Conversely, a more tenuous plasma can strip non-hydrogenic ions resulting in an overestimate in j_i . Unfortunately, a realistic absolute calibration of an intense ion beam Faraday cup is difficult, given the high power density, 100 GW/m^2 or more, of the ion beam. For confidence in this diagnostic, one must rely on earlier comparisons of similar Faraday cup designs with other calibrated beam diagnostics such as particle spectroscopy and Rogowski belt measurements.²⁹ These comparisons typically yield overall confidence levels ranging between ± 20 and $\pm 40\%$.

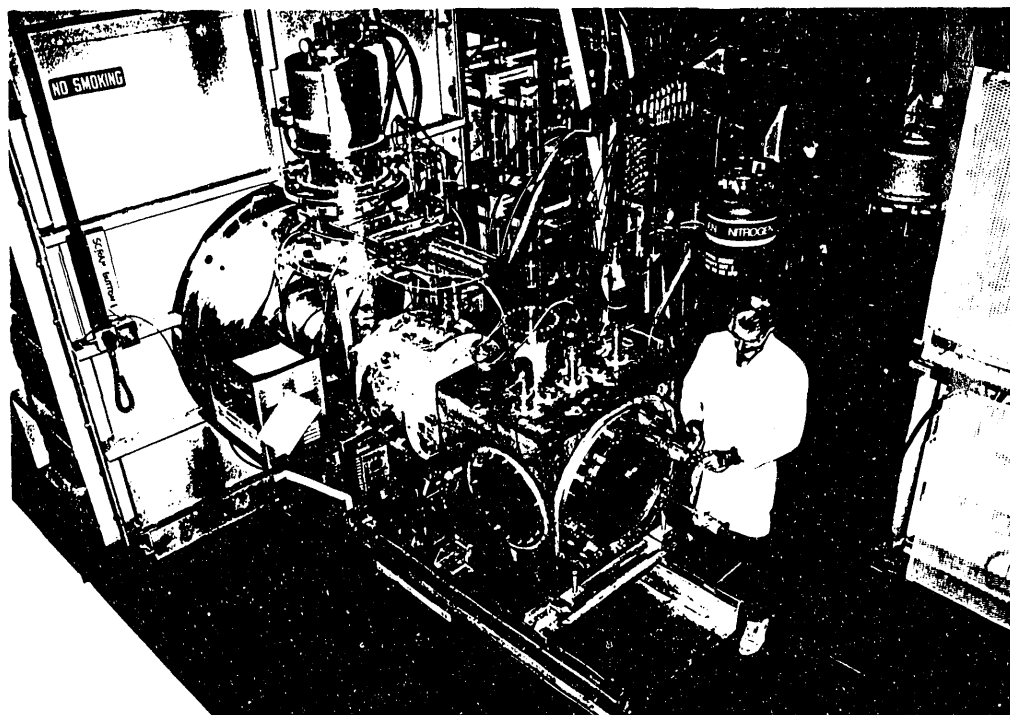


Fig. 6: Photograph of the intense ion beam device.

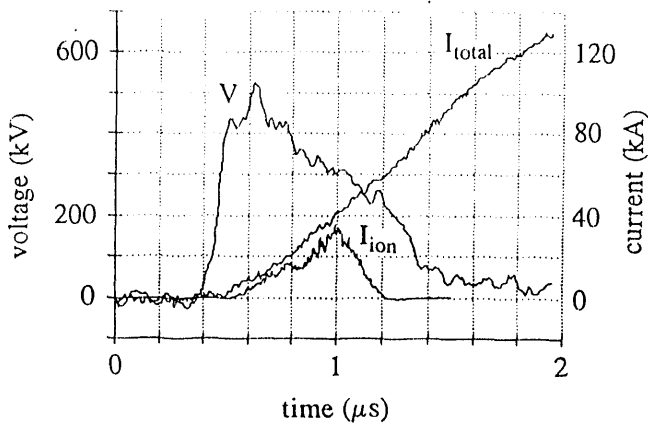


Fig. 7: Typical voltage and current waveforms.

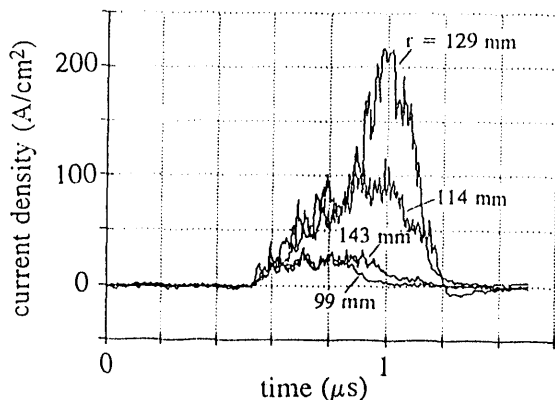


Fig. 8: Typical Faraday cup signals.

Typical waveforms for the diode voltage (with inductive correction) V and current I from a single pulse are shown in Figure 7. The cumulative errors arising from diagnostic and digitizer calibration and noise are estimated at $\pm 7\%$ for V and $\pm 9\%$ for I . Initially, the diode impedance is high, resulting in a voltage risetime that is less than 100 ns. Faraday cup traces are plotted in Figure 8 for the same pulse. Ions are detected starting 200 ns after application of the high-voltage. Ion emission is terminated approximately 600 ns later, presumably due to short circuiting of the diode by expansion of an anode plasma or cathode sheath. The ion emission pulsewidth implies a plasma closure speed of about 25 mm/ μ s, which is consistent with that observed in other devices.^{30,31} The peak ion current of 33 kA is inferred from the product of the anode area and the radially-weighted average of the Faraday cup signals. Further details on the initial ion diode performance may be found elsewhere.¹³

* Permanent Address: Cornell University, Ithaca, NY 14853

Acknowledgment

This research is funded by the USDOE through the Laboratory Directed Research and Development Program at Los Alamos.

References

- [1] V. M. Bystritskii, and A. N. Didenko, *High-Power Ion Beams* (American Institute of Physics, New York, 1989).
- [2] R. N. Sudan, in *Inertial Confinement Fusion*, A. Caruso and E. Sindoni Eds. [Intern. School of Plasma Physics "Piero Caldirola", Italian Phys. Soc., Bologna, 1989], p. 453.
- [3] J. VanDevender, D. Cook, *Science* **232**, 831 (1986); J. VanDevender, *Plasma Phys. and Contr. Fusion* **28**, 841 (1986).

- [4] W. Chu, *et al.*, *Nucl. Instr. and Meth.* **194**, 443 (1982).
- [5] R. Fastow and J. W. Mayer, *J. Appl. Phys.* **61**, 175 (1987).
- [6] Y. Nakagawa *et al.*, *Nucl. Instr. and Meth.* **B39**, 603 (1989).
- [7] A. Progrebnyak *et al.*, *Phys. Stat. Sol. A* **123**, 119 (1991).
- [8] A. N. Didenko *et al.*, *Mat. Sci. and Eng.* **A115**, 337 (1989).
- [9] R. W. Stinnett *et al.*, in *Proc. 1993 IEEE Intern. Conf. on Plasma Science* (IEEE, Piscataway, NJ, 1993) p. 114
- [10] D. S. Phillips, G. P. Johnston, D. J. Rej, R. W. Stinnett, W. J. Waganaar, to be published.
- [11] Y. Shimotori, M. Yokoyama, H. Isobe, S. Harada, K. Masugata, and K. Yatsui, *J. Appl. Phys.* **63**, 968 (1988).
- [12] O. I. Goncharov *et al.*, in *Proc. 8th Intern. Conf. on High-Power Particle Beams*, B. N. Breizman and B. A. Knyazev Editors (World Scientific Publishing Co., Teaneck, NJ, 1991), Vol. II, p. 1243.
- [13] D. J. Rej *et al.*, in *Proc. 9th Intern. Conf. on High-Power Particle Beams*, V. Granstein and D. Mosher Editors (Univ. of Maryland, 1992) in press.
- [14] D. D. Hinshelwood *et al.*, in *Proc. 1993 IEEE Intern. Conf. on Plasma Science* (IEEE, Piscataway, NJ, 1993) p. 116
- [15] Y. Nakagawa, *Japanese J. Appl. Phys.* **23**, 643 (1984).
- [16] D. J. Johnson, J. P. Quintenz, and M. A. Sweeny, *J. Appl. Phys.* **57**, 794 (1985).
- [17] K. Yatsui *et al.*, *Lasers and Particle Beams* **3**, 119 (1985).
- [18] K. Kasuya *et al.*, in *Proc. 8th Intern. Conf. on High-Power Particle Beams*, B. Breizman and B. Knyazev Editors (World Scientific Publishing, Teaneck, NJ, 1991), Vol. I, p. 543.
- [19] H. J. Bluhm *et al.*, *Proc. IEEE* **80**, 995 (1992).
- [20] J. B. Greenly *et al.*, *J. Applied Physics* **63**, 1872 (1988).
- [21] D. A. Hammer *et al.*, in *Proc. 6th Intern. Conf. on High-Power Particle Beams*, B. Yamanaka, Editor (Osaka Univ., Osaka, Japan, 1986), p. 391.
- [22] S. C. Luckhardt and H. H. Fleischmann, *Appl. Phys. Lett.* **30**, 182 (1977).
- [23] D. J. Johnson, T. R. Lockner, *J. Appl. Phys.* **61**, 20 (1987).
- [24] Alloy No. 3, available from Brush-Wellman Inc., Elmhurst, IL 60126.
- [25] Magnets are cast in Stycast 1264 epoxy, available from Emerson and Cuming Inc., Woburn, MA 01888. Pot lifetimes and room-temperature cure times are 3 and 48 hours, respectively. During the casting procedure, the epoxy is mixed, vacuum degassed, and poured into the coil-mold assembly at atmospheric pressure. The assembly is then placed inside an autoclave and evacuated for approximately two hours. Castings are cured for approximately 48 hours in the autoclave at room temperature with an ambient air pressure of approximately 8 atm.
- [26] Pulsed Sciences Inc., San Leandro, CA 94577.
- [27] R. Kraft and B. R. Kusse, *J. Appl. Phys.* **61**, 2123 (1987).
- [28] C. Eichenberger *et al.*, *J. Appl. Phys.* **48**, 1449 (1977).
- [29] C. R. Struckman, PhD Thesis, Cornell University (1992); and D. J. Johnson, personal communication (May 1993).
- [30] C. Litwin and Y. Maron, *Phys. Fluids B* **1**, 670 (1989).
- [31] Y. Kawano *et al.*, *Lasers and Particle Beams* **7**, 277 (1989).

**DATE
FILMED**

8 / 16 / 93

END

